Polyaniline Nano Films Synthesis in One Step *via* Chemical Oxidative Polymerization

Amal Shakir Abbood * 🆔✉, Ibraheem Jaleel Ibraheem 🆔✉

Department of Chemistry, College of Science, University of Anbar, Al-anbar, Iraq.
*Corresponding Author.

Abstract

Polyaniline films were successfully synthesized in this study using an oxidative polymerization method at temperatures ranging from 0 to 4 ° C. Polyaniline films were deposited using a single step of chemical oxidative polymerization rather than electrochemical polymerization. The polyaniline was examined using FTIR, XRD, SEM, AFM, and Four Point Probe. This result demonstrates that polyaniline synthesized using this method has a uniform morphology, small size (17 to 40) nm, high crystallinity, and high conductivity (9.42 s/cm).

Keywords: Atomic Force Microscopy (AFM), Chemical Oxidative Polymerization, Conductive polymers, Polyaniline, X-ray diffraction (XRD).

Introduction

Polyaniline (PANI) a semi-flexible conducting polymer of the organic semiconductor family, as a result of its extraordinary qualities, such as good conductivity, environmental stability, an interesting redox process, low cost starting material, and more [1]. PANI, a conjugated polymer, has been used in a variety of applications across a variety of disciplines, including biosensors [2], supercapacitors [3], actuators [4], electromagnetic interference shielding [5], membranes [6], biofuel cells [7], light-emitting diodes [8], corrosion protection [9], photovoltaic cells [10], solar-cell devices [11], rechargeable batteries [12], field-effect transistors [13], and more.

There are numerous types of polyanilines, each with unique physical and chemical characteristics Fig.1 [14]. They can be categorized as emeraldine, leucoemeraldine, and pernigraniline depending on their oxidation state. For example, pernigraniline is discovered in a fully oxidized state while leucoemeraldine is found in a suitably reduced condition [15].
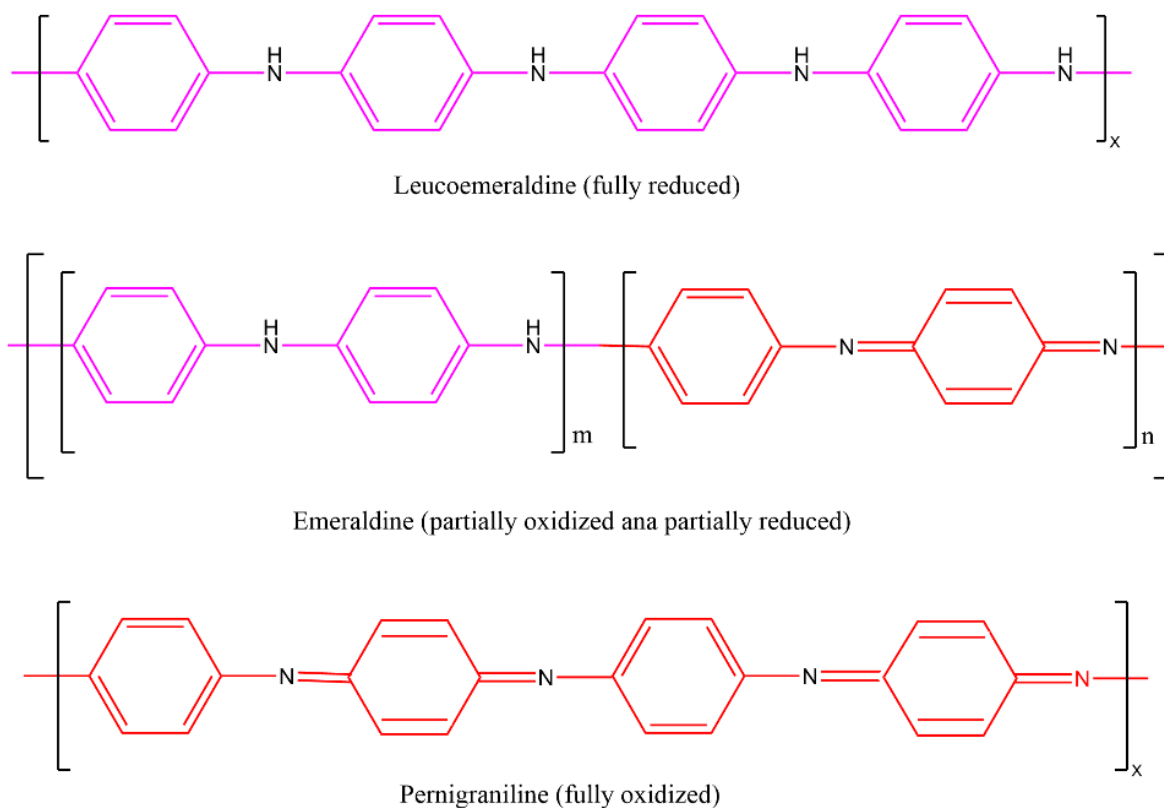
Figure 1. Chemical structure of polyaniline in different oxidation states.

Because nitrogen atoms are involved in the creation of radical cations, unlike most electro conducting polymers whose radical cation is created at carbon, polyaniline conductivity differs from that of other electro conducting polymers. On the other hand, the conjugated double bond system also involves nitrogen. In light of this, polyaniline's electrical conductivity depends on both its oxidation and protonation levels [16-18]. Polyanilines are distinguished by their ability to take on several oxidation forms. To conduct the form of emerald salt, polyaniline in the form of emeraldine base can be doped (protonated). Half-oxidized forms of emeraldine bases include an equal amount of amine (-NH-) and imine (=NH-) sites [19].

In chemical oxidative polymerization (COP), PANI is synthesized using hydrochloric acid (HCl) or sulfuric acid (H_2SO_4) as a dopant and ammonium persulfate (APS) as an oxidant in an aqueous medium [20]. At this time, a proton can be removed by the oxidant from the monomer of aniline without either creating a heavy bond, or with the absolute product [21].

The recommended procedure in this case is the oxidation of monomers to make a cation radical, followed by coupling to create a di-cation and repeating to create a polymer, which is an oxidative coupling [22].

The unique properties of nanoparticles are introduced by a conductive polymer. PANI is related to various properties, including magnetic [23], electrical and dielectric [24], redox [25], anti-corrosion [26], charge–discharge [27], capacitive [28], and sensor properties [29].

The novelty of this research is deposition thin films of polyaniline by one step chemical oxidative polymerization without using electrochemical polymerization.

Materials and Methods

Aniline (99%) was purchased from Merck (Germany), ammonium persulfate (APS) was provided by Aldrich Company. The synthesized polyaniline was characterized by FT-IR spectroscopy/ PerkinElmer, to characterize functional group. X-ray diffraction patterns of the coatings were obtained by employing Philips /X'PERT PRO using CuKα (Kα =1.54056 Å) radiation. Morphological characterization by Field emission scanning electron microscopy (FESEM) and Atomic Force Microscopy (AFM)/ TT-2 AFM Workshop. The electrical conductivity studies were performed using four probe method.

Synthesis of polyaniline

PANI was synthesized by chemical oxidative polymerization of aniline in acidic medium. In a typical procedure, to a 250-mL flask and ITO glass, 100 mL of hydrochloric acid (0.1 M) and 2 mL of Ani (0.021 mol) were added, and the mixture was stirred and cooled down to 0-4 ° C. Then, 0.5 M APS solution (100 mL) was added dropwise within 30 min. The reaction mixture was further stirred for 5 hours at 0–4 ℃ to complete the polymerization as shown in Fig. 2. On completion of reaction, the resulting dark green precipitate was filtered and washed several times with ethanol and deionized water [30], the PANI films was washed also with deionized water. Finally, the resulting PANI was dried over night at 60 ℃ under vacuum.

Aniline (2ml) dissolved in (100ml) of (0.1M) HCl → APS solution is added to Aniline solution → vigorous stirring for 5 hrs. at 0–4 ℃ → precipitate was filtered and washed with Eethanol and DW → PANI film + PANI powder
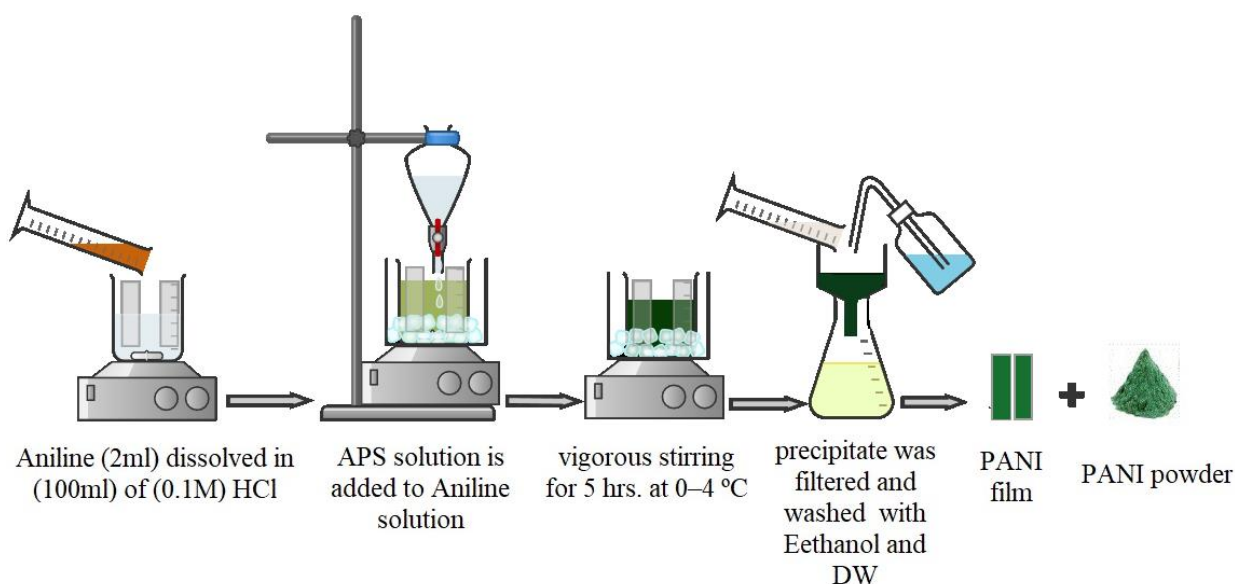
Figure 2. Schematic diagram of synthesizing polyaniline

Results and Discussion

Conductivity Properties

Conductivity of polyaniline thin film was measured at room temperature by a four-probe method, which used for measuring sheet resistance and conductivity, represented in Table 1.

Table 1. Sheet resistance and Conductivity of PANI.

Sheet resistance (KΩ/£)	Conductivity (s/cm)
106.14	9.42

Chemical and Molecular Studies

To study the PANI reaction during chemical oxidation, FTIR spectroscopy was used. Fig. 3 displays the PANI FTIR spectra in the 480–4000 cm^{-1} region. The 1,4-disubstituted benzene ring's out-of-plane vibration, also known as the *para*-coupling structure, is responsible for the 801 cm^{-1} and 507 cm^{-1} peaks. The monosubstituted aromatic ring is the source of the peak at 688 cm^{-1}.

Pure PANI's spectra displayed the typical distinctive stretching vibration bands at 1490 cm^{-1} (C=C, benzenoid rings), and 1562 cm^{-1} (C=C, quinoid rings), 1043, 1076 and 1095 cm^{-1} (C–H) [31], 1126 cm^{-1} (quinone ring stretching vibration), 1200 cm^{-1} (C-N in plane), and 1383 cm^{-1} (aromatic C–N stretch). Due to the existence of (C=N stretching in aromatic), the characteristic peaks at 1460 cm^{-1} and 1557 cm^{-1} are caused by (aromatic C–C stretching). The N-H bend is associated with the 1615 cm^{-1} and 1650 cm^{-1} peak. The peaks at 2326 and 2358 cm^{-1} corresponds to C–N triple band. The peaks at 2875 and 2920 cm^{-1} corresponds to C–H stretching [32].
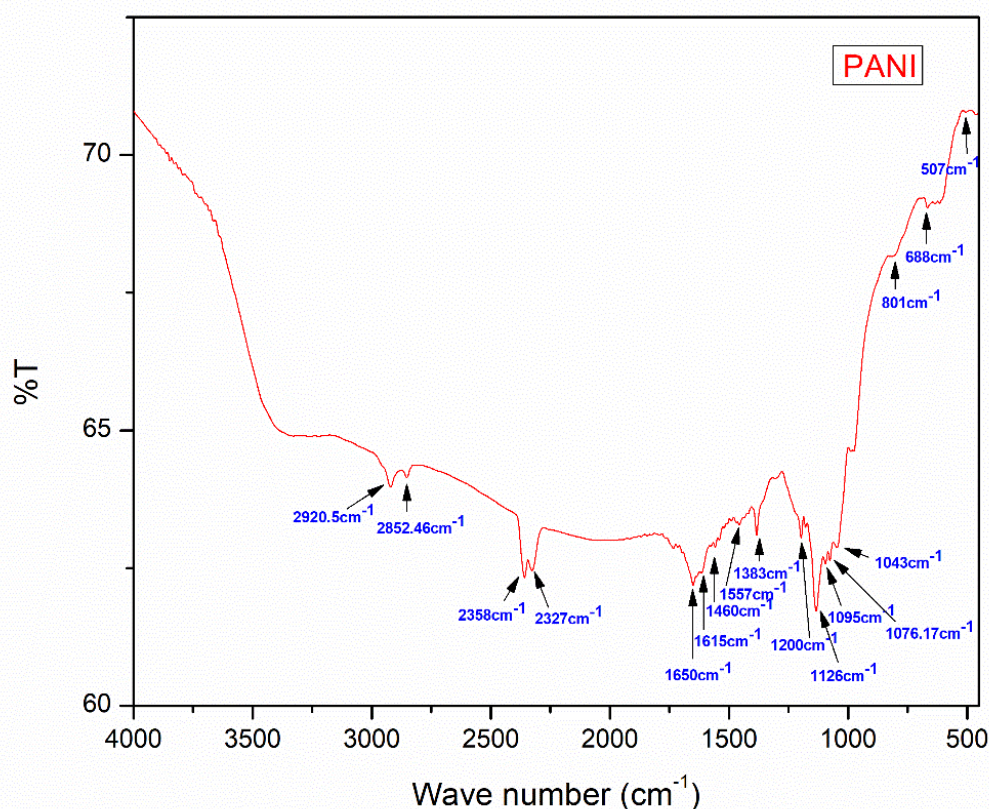

Figure 3. FTIR Spectra of Polyaniline Salt.

XRD analysis of the PANI thin film's crystal structure was performed, and the results are shown in Fig. 4. According to JCPDS card no. 53- 1891, the diffraction peaks found at 2θ = 22.13 degrees and 25.53 degrees, respectively, in this picture demonstrate the amorphous character of PANI (poor crystallinity), and they correspond to 011 and 200 according to the previous studied, respectively [33].

Using the Debye-Scherrer equation, the PANI's grain size is calculated in Eq.1 and the structural parameter of PANI was presented in Table 2.

$$D = \frac{K\lambda}{\beta cos\theta} \quad \ldots\ldots.. 1$$

Where K the Scherrer constant, λ is the light's wavelength utilized for diffraction, β is the sharp peak's complete width at half maximum and θ is the angle being measured". In the calculation above, the Scherrer constant (k), which takes into account the particle's shape, is typically assumed to be 0.9 [34].

Table 2. Structural parameter of PANI.

| No.	2θ (deg)	FWHM (deg)	Cos θ	FWHM (rad)	D (nm)
1	22.1371	1.44000	0.981400924	0.02513089	5.63
2	25.5301	3.92000	0.975287942	0.068411867	2.08
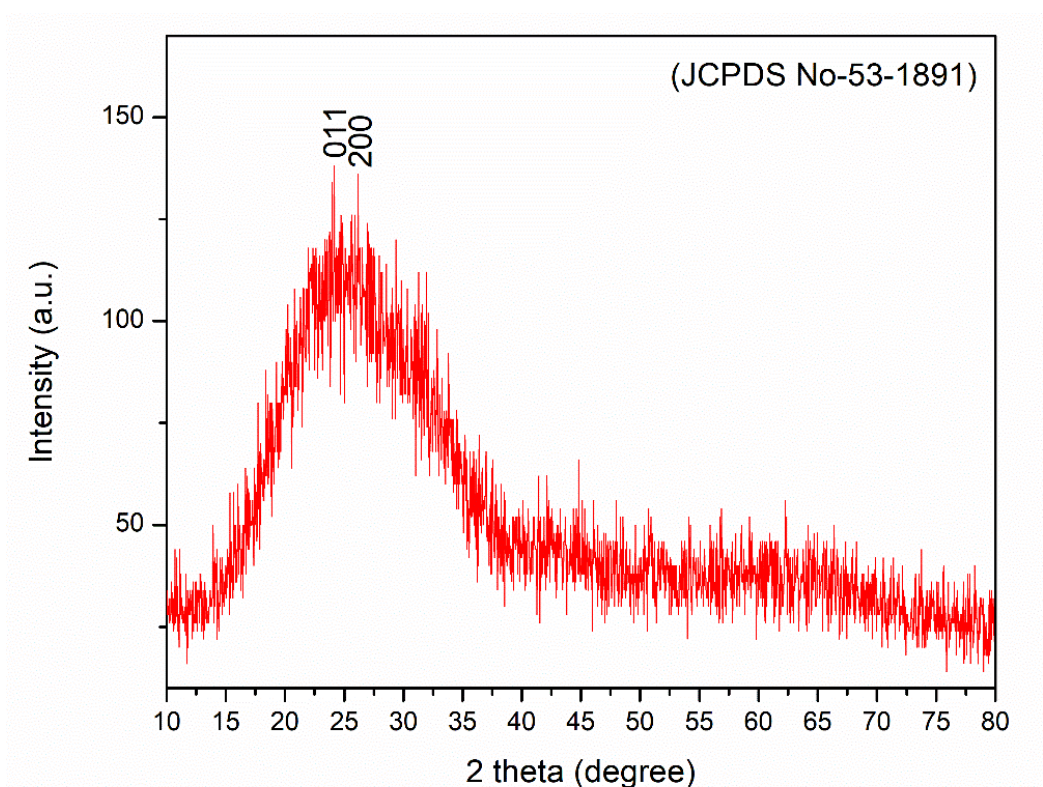
Figure 4. XRD of PANI.

Morphology and Roughness Analysis

FESEM analysis of the surface morphologies of the deposited PANI thin films is depicted in Fig. 5. A and B. The homogeneous deposition of the polymer over the substrate was visible in the FESEM image of the PANI thin films. According to Fig. 5A, these nanotubes have a diameter of 17 to 40 nm and a length of a few micrometers. The surface morphology and roughness of the PANI thin film as-deposited were also examined and measured using AFM. The AFM pictures of the PANI thin films, which demonstrate the deposition of grain-like tubes to generate a thin film, are shown in Fig. 5 C. These results are in line with the SEM pictures, which also showed comparable morphologies. The PANI films' surface roughness was determined to be 7.715 nm as shown in Table 3. When the substrate was already present in the reaction before the addition of an initiator, such as APS solution, uniform film deposition could be observed. The thickness of the films was significantly reduced if the substrate was added during the induction period, which is between one and three minutes after the polymerization began. Similar to this, if the substrate was added after 6-7 min, no films were formed because aniline cation radicals, which are necessary for primary nucleation, were not present. In order to generate high-quality and stable films with a corresponding surface roughness of 7.715 nm, the substrate has to be added before polymerization.
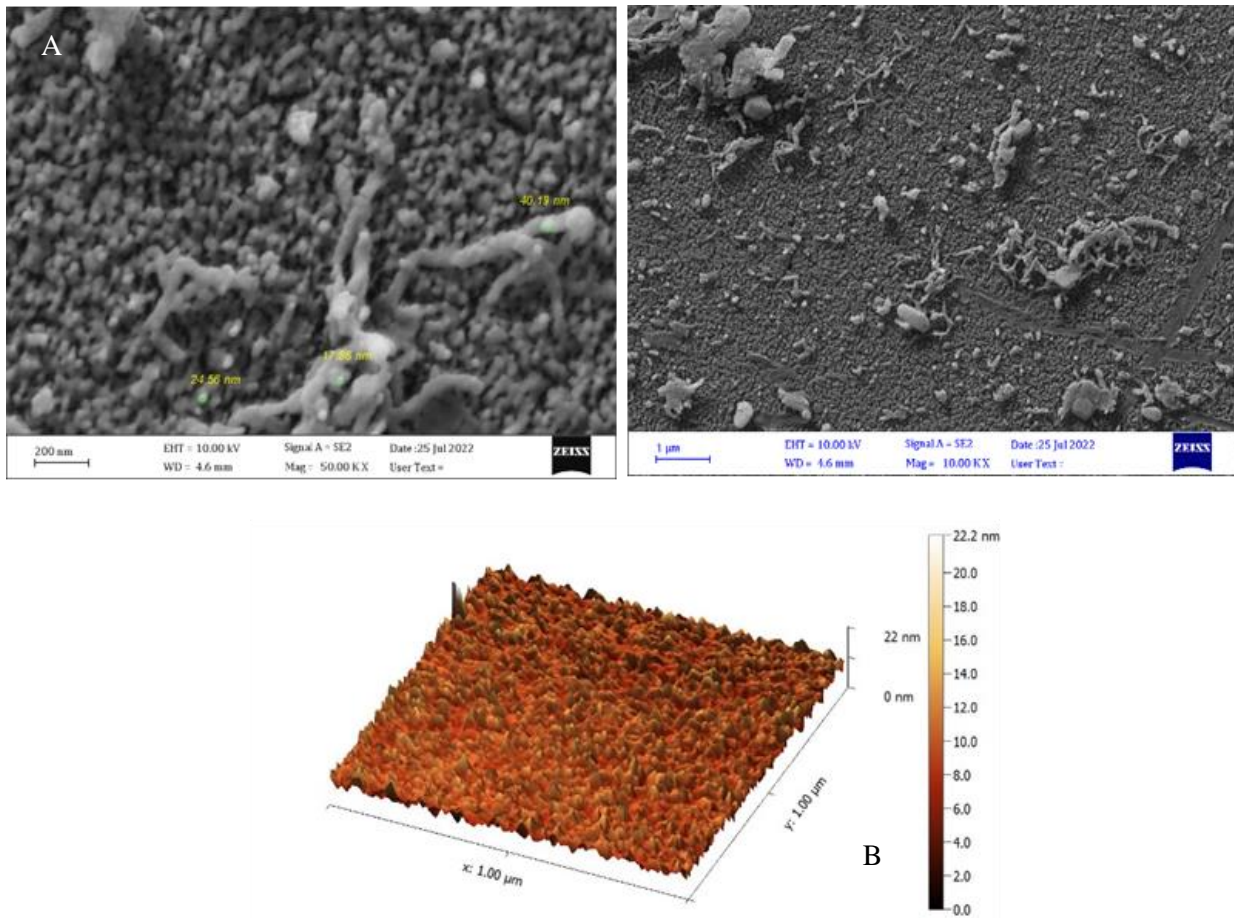
**Figure 5. (A): FESEM Photograph of Polyaniline 200 nm
(B): FESEM Photograph of Polyaniline 1 μm
(C) AFM images of Polyaniline**

Table 3. Summary of the AFM information of PANI.

Roughness Average	Root Mean Square	Ten Point High	Average Diameter
Sa (nm)	Sq (nm)	Sz (nm)	D (nm)
7.715	10.45	74.12	62.91

Using cyclic voltammetry, the electrochemical behavior of the PANI thin film as-deposited was examined. The pH of the solution, NaOH, was set to 8.0, and measurements were made in the potential range of 0.0 V to 0.8 V at 10 mV s^{-1}. The cyclic voltammograms of PANI films are displayed in Fig. 6. These oxidation and reduction peaks were seen at 0.64 V and 0.2 V, respectively (vs. the reference electrode). These sustained redox and oxidant peaks are a result of the PANI's high conductivity.
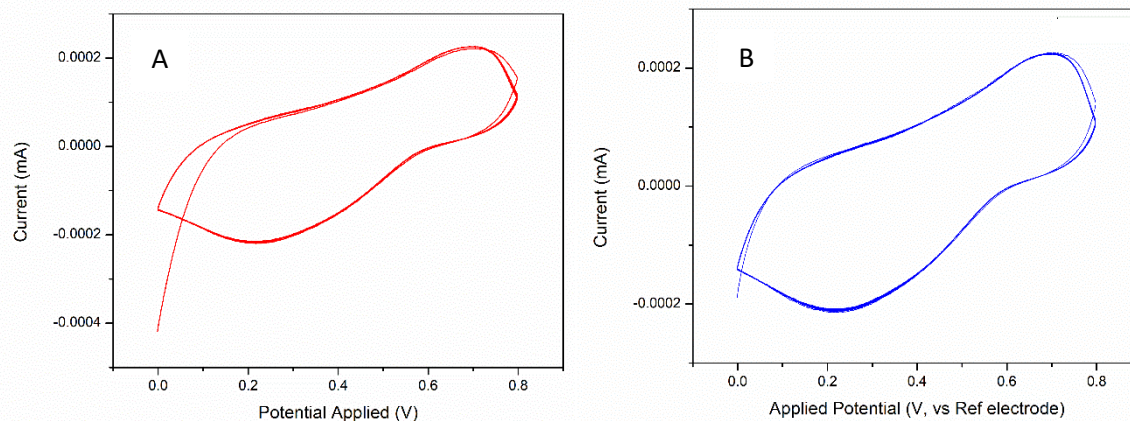
Figure 6. CV of PANI film at (A) 5 Cycles (B) 15 Cycles.

Conclusion

We conclude from this research that the concentration of the acid and the temperature at 0-4 ° C for about 6 hours and amount of oxidant lead to formation nanotube of polyaniline and deposit it directly on the ITO glass substrate with the dimeter of 17 to 40 nm and roughness of 7.715 nm.

Acknowledgment

Authors' Declaration

- Conflicts of Interest: None.
- We hereby confirm that all the Figures and Tables in the manuscript are ours. Furthermore, any Figures and images, that are not ours, have been included with the necessary permission for re-publication, which is attached to the manuscript.

- Authors sign on ethical consideration's approval.
- Ethical Clearance: The project was approved by the local ethical committee in University of Anbar.

Authors' Contribution Statement

A. S. A. conceived of the presented idea, carried out the experiment, wrote the manuscript, and performed the analysis and discussed the results and contributed to the final manuscript. I. J. I. supervised the project.

References

1. Abel SB, Yslas EI, Rivarola CR, Barbero CA. Synthesis of polyaniline (PANI) and functionalized polyaniline (F-PANI) nanoparticles with controlled size by solvent displacement method. Application in fluorescence detection and bacteria killing by photothermal effect. Nanotechnol. 2018 Feb 9;29(12):125604. https://doi.org/10.1088/1361-6528/aaa99a.

2. Othman SA. Conjugated Polymer of Biosensor using Langmuir-Blodgett Technique-A Review. J. Phys: Conference Series 2022 ;2169(1):012030). https://doi.org/10.1088/1742-6596/2169/1/012030

3. Cho S, Lee JS, Joo H. Recent developments of the solution-processable and highly conductive polyaniline composites for optical and electrochemical applications. Polymers. 2019 Nov 29;11(12):1965. https://doi.org/10.3390/polym11121965

4. Qian C, Li Y, Chen C, Han L, Han Q, Liu L, Lu Z. A stretchable and conductive design based on multi-responsive hydrogel for self-sensing actuators. Chem

Eng J. 2023 Feb 15; 454:140263. https://doi.org/10.1016/j.cej.2022.140263.

5. Das P, Deoghare AB, Maity SR. Synergistically improved thermal stability and electromagnetic interference shielding effectiveness (EMI SE) of in-situ synthesized polyaniline/sulphur doped reduced graphene oxide (PANI/S-RGO) nanocomposites. Ceram Int. 2022 Apr 15;48(8):11031-42. https://doi.org/10.1016/j.ceramint.2021.12.323

6. Luangaramvej P, Poungsripong P, Dubas ST. Synthesis of Janus polyaniline–polyelectrolyte complex membrane via in situ confined polymerization. Polym Int. 2022 Jan;71(1):139-45. https://doi.org/10.1002/pi.6294

7. Guan HS, Song WZ, Huang LP, Liu Z, Zhang J, Ramakrishna S, et al. Artificial blood vessel biofuel cell for self-powered blood glucose monitoring. Nanotechnol. 2021 Oct 22;33(2):025404. https://doi.org/10.1088/1361-6528/ac2d47

8. Faraco TA, de Lima Fontes M, Paschoalin RT, Claro AM, Gonçalves IS, Cavicchioli M, de Farias RL, Cremona M, Ribeiro SJ, da Silva Barud H, Legnani C. Review of Bacterial Nanocellulose as Suitable Substrate for Conformable and Flexible Organic Light-Emitting Diodes. Polymers. 2023 Jan;15(3):479. https://doi.org/10.3390/polym15030479.

9. Kumar AM, Jose J, Hussein MA. Novel polyaniline/chitosan/reduced graphene oxide ternary nanocomposites: Feasible reinforcement in epoxy coatings on mild steel for corrosion protection. Prog Org Coat. 2022 Feb 1; 163:106678. https://doi.org/10.1016/j.porgcoat.2021.106678

10. Mohseni HR, Dehghanipour M, Dehghan N, Tamaddon F, Ahmadi M, Sabet M, et al. Enhancement of the photovoltaic performance and the stability of perovskite solar cells via the modification of electron transport layers with reduced graphene oxide/polyaniline composite. Sol Energy. 2021 Jan 1; 213:59-66. https://doi.org/10.1016/j.solener.2020.11.017

11. Kim DI, Lee JW, Jeong RH, Boo JH. A high-efficiency and stable perovskite solar cell fabricated in ambient air using a polyaniline passivation layer. Sci Rep. 2022 Jan 13;12(1):1-0. https://doi.org/10.1038/s41598-021-04547-3

12. Zhang Y, Xu L, Jiang H, Liu Y, Meng C. Polyaniline-expanded the interlayer spacing of hydrated vanadium pentoxide by the interface-intercalation for aqueous rechargeable Zn-ion batteries. J Colloid Interface Sci. 2021 Dec 1; 603:641-50. https://doi.org/10.1016/j.jcis.2021.06.141

13. Mello HJ, Junior BB, Mulato M. Polyaniline-based field effect transistor for DNA/RNA biomarker sensing: Comparison to electrochemical impedance

and inorganic layer. Sens Actuators A Phys 2021 Feb 1; 318:112481. https://doi.org/10.1016/j.sna.2020.112481

14. Namsheer K, Rout CS. Conducting polymers: A comprehensive review on recent advances in synthesis, properties and applications. RSC Adv. 2021;11(10):5659-97. https://doi.org/10.1039/D0RA07800J

15. Al-Zohbi F. A Review of Tailoring Polyaniline Ionic Liquids for Long Cycle-Stable Supercapacitors with High Capacitance. J. Chem. Rev. 2023;5(2):143-58. https://doi.org/10.22034/JCR.380607.1206.

16. Bubniene US, Ratautaite V, Ramanavicius A, Bucinskas V. Conducting Polymers for the Design of Tactile Sensors. Polymers. 2022 Jul 23;14(15):2984. https://doi.org/10.3390/polym14152984.

17. Fedorko P, Trznadel M, Pron A, Djurado D, Planès J, Travers JP. New analytical approach to the insulator–metal transition in conductive polyaniline. Synth Met. 2010 Aug 1;160(15-16):1668-71. https://doi.org/10.1016/j.synthmet.2010.05.038

18. Pron A, Rannou P. Processible conjugated polymers: from organic semiconductors to organic metals and superconductors. Prog Polym Sci. 2002 Feb 1;27(1):135-90. https://doi.org/10.1016/S0079-6700(01)00043-0

19. Hasoon SA, Abdul-Hadi SA. Optical, structural and electrical properties of electrochemical synthesis of thin film of polyaniline. Baghdad Sci.J. 2018;15(1). http://dx.doi.org/10.21123/bsj.2018.15.1.0073

20. Boudjelida S, Djellali S, Ferkous H, Benguerba Y, Chikouche I, Carraro M. Physicochemical Properties and Atomic-Scale Interactions in Polyaniline (Emeraldine Base)/Starch Bio-Based Composites: Experimental and Computational Investigations. Polymers. 2022 Apr 7;14(8):1505. https://doi.org/10.3390/polym14081505.

21. Beygisangchin M, Abdul Rashid S, Shafie S, Sadrolhosseini AR, Lim HN. Preparations, properties, and applications of polyaniline and polyaniline thin films—A review. Polymers. 2021 Jun 18;13(12):2003. https://doi.org/10.3390/polym13122003

22. Sangamesha MA, Pushpalatha K, Shekar GL. Synthesis and characterization of conducting polyaniline/copper selenide nanocomposites. Indian J. Adv. Chem. Sci. 2014;2(3):223-7. ID:41704482.

23. Pal R, Goyal SL, Rawal I, Gupta AK. Tailoring of EMI shielding properties of polyaniline with MWCNTs embedment in X-band (8.2–12.4 GHz). J. Phys. Chem. Solids. 2022 Oct 1;169:110867. https://doi.org/10.1016/j.jpcs.2022.110867.

24. Qasim KF, Mousa MA. Electrical and dielectric properties of self-assembled polyaniline on barium

sulphate surface. Egypt. J. Pet.. 2021 Dec 1;30(4):9-19. https://doi.org/10.1016/j.ejpe.2021.09.001

25. Alipanah N, Dehghani A, Abdolmaleki M, Bahlakeh G, Ramezanzadeh B. Designing environmentally-friendly pH-responsive self-redox polyaniline grafted graphene oxide nano-platform decorated by zeolite imidazole ZIF-9 MOF for achieving smart functional epoxy-based anti-corrosion coating. J. Environ. Chem. Eng. 2023 Feb 1;11(1):109048. https://doi.org/10.1016/j.jece.2022.109048.

26. Wu K, Gui T, Dong J, Luo J, Liu R. Synthesis of robust polyaniline microcapsules via UV-initiated emulsion polymerization for self-healing and anti-corrosion coating. Prog Org Coat. 2022 Jan 1;162:106592. https://doi.org/10.1016/j.porgcoat.2021.106592

27. Thanasamy D, Jesuraj D, Avadhanam V, Chinnadurai K, Kannan SK. Microstructural effect of various polyaniline-carbon nanotube core-shell nanocomposites on electrochemical supercapacitor electrode performance. J Energy Storage. 2022 Sep 1; 53:105087. https://doi.org/10.1016/j.est.2022.105087

28. Fu F, Wang H, Yang D, Qiu X, Li Z, Qin Y. Lamellar hierarchical lignin-derived porous carbon activating the capacitive property of polyaniline for high-performance supercapacitors. J Colloid Interface Sci. 2022 Jul 1; 617:694-703. https://doi.org/10.1016/j.jcis.2022.03.023

29. Shen Y, Zheng L. Polyaniline-poly (methylene blue) nano-rod composites as an electrochemical sensor for sensitive determination of ascorbic acid. Int. J. Electrochem. Sci. 2023 Jan 1;18(1):6-12. https://doi.org/10.1016/j.ijoes.2023.01.007

30. Solonaru AM, Asandulesa M, Honciuc A. Homologous Series of Polyaniline Derivatives Block Copolymers with Amphiphilic and Semiconducting Properties. Polymers. 2022 May 25;14(11):2149. https://doi.org/10.3390/polym14112149.

31. Wang R, Jing Y. The effect of inorganic salt on the morphology and nucleation of polyaniline nanofibers synthesized via self-assembly. Des. Monomers Polym. 2023 Dec 31;26(1):45-53. https://doi.org/10.1080/15685551.2023.2166727.

32. Mahinnezhad S, Izquierdo R, Shih A. Fully Printed pH Sensor based on Polyaniline/Graphite Nanocomposites. J. ElectroChem. Soc. 2023 Jan 24. https://doi.org/10.1149/1945-7111/acb5c3.

33. Gamal A, Shaban M, BinSabt M, Moussa M, Ahmed AM, Rabia M, et al. Facile Fabrication of Polyaniline/Pbs Nanocomposite for High-Performance Supercapacitor Application. Nanomaterials. 2022 Feb 28;12(5):817. https://doi.org/10.3390/nano12050817

34. Abbood A. Synthesis of C60 Nanotube from Pyrolysis of Plastic Waste (Polypropylene) with Catalyst. Baghdad Sci.J. 2020 Jun 21;17(2 (SI)):0624-. https://doi.org/10.21123/bsj.2020.17.2(SI).0624.

تحضير أفلام البولي انيلين بخطوة واحدة بواسطة البلمرة الكيميائية المؤكسدة

امال شاكر عبود[1]، ابراهيم جليل ابراهيم[2]

قسم الكيمياء، كلية العلوم، جامعة الأنبار، الأنبار، العراق.

الخلاصة

تم تصنيع أغشية البولي انيلين بنجاح في هذه الدراسة باستخدام طريقة البلمرة المؤكسدة بدرجات حرارة تتراوح من 0-4 درجة مئوية. تم ترسيب أغشية البولي انيلين بأستخدام خطوة واحدة من البلمرة المؤكسدة الكيميائية بدلا من البلمرة الكهروكيميائية. تم تشخيص البولي انيلين بأستخدام FTIR، XRD، SEM، AFM، وFour Point Probe. أظهرت النتائج أن البولي انيلين الذي تم تصنيعه بهذه الطريقة كان ذو شكل موحد، وحجم صغير(17الى40) نانومتر، وتبلور كبير، وموصلية عالية (9.42 سيمنزلكل سم).

الكلمات المفتاحية: مجهر القوة الذرية، البلمرة الكيميائية المؤكسدة، البوليمرات الموصلة، بولي انيلين، حيود الاشعة السينية.